

Toxicology Research

Accepted Manuscript



This is an *Accepted Manuscript*, which has been through the Royal Society of Chemistry peer review process and has been accepted for publication.

Accepted Manuscripts are published online shortly after acceptance, before technical editing, formatting and proof reading. Using this free service, authors can make their results available to the community, in citable form, before we publish the edited article. We will replace this *Accepted Manuscript* with the edited and formatted *Advance Article* as soon as it is available.

You can find more information about *Accepted Manuscripts* in the [Information for Authors](#).

Please note that technical editing may introduce minor changes to the text and/or graphics, which may alter content. The journal's standard [Terms & Conditions](#) and the [Ethical guidelines](#) still apply. In no event shall the Royal Society of Chemistry be held responsible for any errors or omissions in this *Accepted Manuscript* or any consequences arising from the use of any information it contains.

Full Title

Cytotoxic and Sublethal Effects of Silver Nanoparticles on Tendon-derived Stem Cells – Implications for Tendon Engineering

Author's Name and Affiliations

Tik Shing Cheung^a; Pui Man Lau^a; Haifei Lu^b; Ho Pui Ho^b; Pauline Po Yee Lui^c and Siu Kai Kong^{a*}

^a Program of Biochemistry, School of Life Sciences, The Chinese University of Hong Kong, Hong Kong

^b Department of Electronic Engineering, Center for Advanced Research in Photonics, The Chinese University of Hong Kong, Hong Kong

^c Headquarter, Hospital Authority, Hong Kong

*To whom correspondence should be addressed at Program of Biochemistry, School of Life Sciences, The Chinese University of Hong Kong, Hong Kong. Fax: (852) 2603 5123. Telephone: (852) 3943 6799. E-mail: skkong@cuhk.edu.hk

Abstract

Tendon injuries occur commonly in sports and workplace. Tendon-derived stem cells (TDSCs) have great potential for tendon healing because they can differentiate into functional tenocytes. To grow TDSCs properly *in vivo*, a scaffold is needed. Silver nanoparticles (AgNPs) have been used in a range of biomedical applications for their anti-bacterial and -inflammatory effects. AgNPs are therefore expected to be a good scaffolding coating material for tendon engineering. Yet, their cytotoxicity in TDSCs remains unknown. Moreover, their sublethal effects were mysterious in TDSCs. In our study, decahedral AgNPs (43.5 nm in diameter) coated with polyvinylpyrrolidone (PVP) caused a decrease in TDSCs' viability beginning at 37.5 $\mu\text{g/ml}$ but showed non-cytotoxic effects at concentrations below 18.8 $\mu\text{g/ml}$. Apoptosis was observed in the TDSCs when higher doses of AgNPs (75-150 $\mu\text{g/ml}$) were used. Mechanistically, AgNPs induced reactive oxygen species (ROS) formation and mitochondrial membrane potential (MMP) depolarization, resulting in apoptosis. Interestingly, treating TDSCs with N-acetyl-L-cysteine (NAC) antioxidant significantly antagonized the ROS formation, MMP depolarization and apoptosis indicating that ROS accumulation was a prominent mediator in the AgNPs-induced cytotoxicity. On the other hand, AgNPs inhibited the tendon markers mRNA expression (0-15 $\mu\text{g/ml}$), proliferation and clonogenicity (0-15 $\mu\text{g/ml}$) in TDSCs under the non-cytotoxic concentrations. Taken together, we reported here for the first time that the decahedral AgNPs were cytotoxic to rat TDSCs and their sublethal effects were also detrimental to stem cells' proliferation and tenogenic differentiation. Therefore, AgNPs were not a good scaffolding coating material for tendon engineering.

Keywords

Silver nanoparticles (AgNPs), tendon-derived stem cells (TDSCs), tendon engineering, cytotoxicity, oxidative stress, sublethal effects

Abbreviations

AgNPs, silver nanoparticles;

AgNO₃, silver nitrate;

BMSCs, bone marrow-derived mesenchymal stem cells;

CM-H₂DCFDA, chloromethyl derivative of 2',7'-dichlorodihydrofluorescein diacetate

Col1A1, collagen type 1 alpha-1;

Col3A1, collagen type 3 alpha-1;

DLS, dynamic light scattering;

FESEM, field-emission scanning electron microscopy;

FSC, forward scatter;

IC₅₀, half maximum inhibitory concentration;

MMP, mitochondria membrane potential;

MTT, 3-(4,5-Dimethylthiazol-2-yl)-2,5-Diphenyltetrazolium bromide;

NAC, N-acetyl-L-cysteine;

PI, propidium iodide;

PS, phosphatylserine;

PVP, polyvinylpyrrolidone;

RT-qPCR, real time quantitative reverse transcription polymerase chain reaction;

ROS, reactive oxygen species;

Scx, scleraxis;

SSC, side scatter;

TDSC, tendon-derived stem cell;

TEM, transmission electron microscopy;

Tnmd, tenomodulin;

Introduction

Tendon injuries are common in many physical activities¹. Injured tendons do not fully heal but frequently form fibrotic scars^{1,2}. Traditional therapies for tendon injuries include artificial implants, autograft, or allograft transplantation; but all of these have various limitations such as short serviceable life, low biocompatibility, risks of immune rejection and bacterial infection³. To improve the quality of tendon healing, tendon engineering has been an emerging alternative to patients with tendon injuries. Among different sources of cells for tendon engineering, tendon-derived stem cells (TDSCs) have been progressively mentioned because of their functional advantages⁴⁻⁶. TDSCs were discovered in tendons and identified in human, mouse⁷ and rat⁸. They have a higher proliferation rate, clonogenicity, and stronger *in vitro* multi-lineage differentiation potential when compared to that of the marrow-derived mesenchymal stem cells (BMSCs)⁹. More importantly, our recent findings showed that transplantation of allogeneic TDSCs to the patellar tendon window wound exhibited better healing outcomes, lower immunogenicity, and weaker host immune-rejection in the recipient animals^{10,11}.

Along with this development, the field of nanomaterials has been advancing rapidly for bio-scaffold fabrication in tissue engineering. Among the nanomaterials, silver nanoparticle (AgNPs), defined as the clusters of silver atoms ranging in diameter from 1 to 100 nm¹², have gained much attention for their unique properties. For example, AgNPs are able to destroy a wide range of bacteria^{13,14}, alleviate inflammation^{15,16}, and accelerate wound healing process^{17,18}. Hence, AgNPs have been widely used in medical device coating¹⁹ and venous catheters¹². Given the superiority of AgNPs, they were used for fabricating nano-scaffolds in attempt to deal with bacterial infections occurred during transplantation^{20,21}. Alt

et al (2014) synthesized polymethylmetacrylate bone cement loaded with AgNPs (5–50 nm in diameter) and reported that these AgNPs-coated scaffolds exhibited potent anti-bacterial effects against several strains of bacteria without causing cytotoxicity in mammalian cells²¹. Moreover, there was a recent pre-clinical study demonstrating that nano-scaffold containing AgNPs significantly accelerated wound healing *in vivo* and inhibited bacteria growth *in vitro*²². Based on these studies, there is an increasing interest in exploring the possibility of using AgNPs as the carrier or scaffolding material to deliver stem cells to the injury site to improve the tendon healing process as described by Karthikeyan *et al*²³.

However, it still remains unknown if AgNPs are able to be a good scaffold material without causing any toxic effects on TDSCs in tendon engineering. Some studies showed that AgNPs have cytotoxic and apoptotic effects in different cell types^{24–26}. Although assessments demonstrating how AgNPs affect cells and animals are rising, it is difficult to conjecture the availability of AgNPs in TDSCs because toxicity of AgNPs may vary in different cells. Even worse, most studies lacked proper characterization of the AgNPs, making it difficult to conclude the availability of AgNPs²⁷. More importantly, a recent review has indicated that most research articles and review only discussed the toxicity of AgNPs at high-concentration exposure but not the sublethal doses, which are the relatively low concentrations of AgNPs without eliciting apparent cytotoxicity²⁸. In fact, sublethal doses of AgNPs are more relevant to the actual doses of AgNPs used in medical applications and doses of AgNPs exposed in the environment. To have a better understanding of the harmful effects of AgNPs, toxicities of sublethal AgNPs on cells, animals or even human have to be elucidated.

To determine if AgNP was a suitable scaffolding material in tendon engineering, one major objective of this study was to clarify, for the first time, the impact of AgNPs on TDSCs'

viability, proliferation and tenogenic differentiation. We concluded that doses of AgNPs were divided into sublethal range and lethal range based on the result of dose-dependent curve of AgNPs against TDSCs' viability after 24-hour incubation. Then, lethal doses of AgNPs (e.g. >37.5 $\mu\text{g/ml}$) were used to investigate the toxicological mechanism of AgNPs in TDSCs using annexin-V & propidium iodide (PI) assay, JC-1 assay and reactive oxygen species (ROS) CM-H₂DCFDA assay while sublethal doses of AgNPs (e.g. <18.8 $\mu\text{g/ml}$) were used to examine the chronic effects of AgNPs on proliferation and tenogenic differentiation.

Experimental

Synthesis of AgNPs

AgNPs were synthesized photochemically following the steps as described previously²⁹. Briefly, sodium citrate (0.05 M, 4 ml) was initially mixed with PVP (0.05 M, 0.7 ml) and 80 ml water. Subsequently, L-arginine (0.01 M, 0.3 ml), silver nitrate (0.04 M, 0.225 ml) and sodium borohydride (0.1 M, 1 ml) were added into the mixture with continuous stirring for 30 min. Next, the solution was incubated at room temperature for 3 h in a dark environment. The bright yellow solution was then exposed to a blue LED (6 V, 400 mA, and 3 W) for 15 h. Under the exposure to blue light, the silver ions were reduced by sodium borohydride to form decahedron particles and coated with polyvinylpyrrolidone (PVP). Sodium citrate plays a role as stabilizers and arginine functions as a photochemical promoter. The final concentration of AgNPs suspension was 4.5 µg/ml. The mass of silver nanoparticle here was referring to the mass of silver in the nanoparticle. AgNPs were pelleted by centrifugation at 12,000 rpm (Eppendorf, Hamburg, Germany) for 10 min and resuspended in DMEM containing 10% (v/v) fetal bovine serum (FBS) and 1% (v/v) penicillin-streptomycin (P-S) to a desired concentration for assays.

Physicochemical characterization of AgNPs

Field-emission scanning electron microscopy (FESEM) was performed using a Carl Zeiss Ultra Plus FESEM (CA, USA) and the operating voltage was 4.96 kV, while transmission electron microscopy (TEM) was performed using a FEI CM120 microscope (Oregon, USA) at 120 kV. The average edge length of AgNPs was determined from the SEM and TEM

images of at least 100 AgNPs (Lu et al. 2012). The average diameter of AgNPs was then calculated. Hydrodynamic diameters of AgNPs in water and complete DMEM were determined by dynamic light scattering (DLS) using a modified commercial LLS spectrometer (ALV/ SP-125 equipped with an ALV-5000 multi-tau digital time correlator) with a solid-state laser (ADLAS DPY42511, output power is 400 MW at 532 nm) as the light source. The size and homology of AgNPs was monitored by UV–visible spectroscopy (ELISA microplate reader, Bio-Rad, USA) at the wavelength of 495nm.

Isolation and culture of TDSCs

The isolation of TDSCs from rats was approved by the Animal Research Ethics Committee, The Chinese University of Hong Kong, under a research project entitled “Mesenchymal stem cells (MSCs) for tendon regeneration” (Ref. No. 10/105/MIS). TDSCs were isolated and prepared from the mid-substances of patellar tendon of 8-week old Sprague-Dawley rats (gender, weight: 250-320 g) as described previously^{8-10,30}. Briefly, after euthanasia, the mid-substances of both patellar tendons were excised. Care was taken that only the mid-substance of patellar tendon tissue, but not the tissue at the tendon-bone junction, was collected. The peritenon was carefully removed and the tissue was stored in sterile phosphate-buffered saline (PBS). The tissue was minced, digested with 3 mg/ml type I collagenase (Sigma-Aldrich, St. Louis, MO, USA) and passed through a 70 µm cell strainer (Becton Dickinson, Franklin Lakes, USA) to yield a single-cell suspension. The released cells were washed in PBS and resuspended in DMEM containing 10% (v/v) FBS and 1% (v/v) P-S (All from Invitrogen Corporation, Carlsbad, USA). The isolated nucleated cells were plated at an optimal low cell density of 500 cells/cm² for the isolation of TDSCs and cultured at 37°C, 5% CO₂ to form colonies. At day 2 after initial plating, the cells were washed twice with PBS

to remove the non-adherent cells. After one week, the cell colonies were trypsinized and pooled as passage 0 (P0). P0 cells were subsequently expanded at the same seeding density (500 cells/cm²). The isolated cells expressed stem cell-related surface markers including CD90, CD73 and CD44 and were negative for CD45 and CD31 as shown by flow cytometry (results not shown). TDSCs at passage 3-5 were used for the assays in this study.

MTT viability assay

The effect of AgNPs and silver nitrate (AgNO₃) on the viability of TDSCs was assessed using the MTT assay. TDSCs were seeded at 10⁴ cells/well in DMEM in 96-well plates overnight at 37°C, 5% CO₂. The TDSCs were then treated with AgNPs in DMEM (0-150 µg/ml) for 24 h. MTT solution in PBS (5 mg/ml, 20 µl) was then added to each well and the cells were incubated for another 2.5 h. The cells were then permeabilized and the formazan crystals were dissolved in 100 µl of dimethylsulphoxide (DMSO). The absorbance at 550 nm was measured using an ELISA microplate reader (Bio-Rad, USA). Because of the interference of the AgNPs³¹, the background absorbance of each corresponding control was subtracted from the experimental groups. The percentages of viable cells after treatment with various concentrations of AgNPs were determined. Triplicate sets of experiment were examined.

Cellular morphological change

TDSCs were treated with different concentrations of AgNPs (0-150 µg/ml) in DMEM for 24 h at 37°C, 5% CO₂. The changes of cell morphology upon AgNPs treatment were observed using an optical inverted microscope (Nikon TE 2000, NY, USA).

Toxicological mechanisms of lethal AgNPs in TDSCs

Cellular uptake of AgNPs

The uptake of AgNPs into cells was determined by measuring the change in side scatter (SSC) signal in flow cytometric analysis³². Briefly, TDSCs were treated with different concentrations of AgNPs (0-150 µg/ml) in DMEM for 24 h at 37°C, 5% CO₂. The forward scatter (FSC) and side scatter (SSC) signals of TDSCs after treatment were then determined by a flow cytometer (Becton Dickinson Biosciences, NJ, USA). Ten thousand events were counted. The increase in SSC signals in the experimental groups relative to the control group provided an estimation of the amount of AgNPs taken up into the cells³². The percentages of cells in the selected high SSC region in different groups were presented in a bar chart. Triplicate sets of experiment were examined.

Annexin-V-GFP and PI apoptotic assay

The apoptotic effect of AgNPs on TDSCs was assessed by double staining the cells with annexin-V-GFP/PI. After treatment with AgNP (0-150 µg/ml) for 24 h at 37°C, 5% CO₂, TDSCs in suspension were labeled with annexin-V-GFP and PI (final concentration 4 µg/ml) in dark for 15 min at room temperature. 10,000 events were analyzed by flow cytometry. The percentages of early apoptotic cells (annexin-V-GFP_{High}; PI_{Low}), and late/necrotic cells (annexin-V-GFP_{High}; PI_{High}) in the dot plots were determined. TDSCs treated with digitonin (40 µg/ml), which permeabilizes the cell membrane, was used to set the quadrants for the viable, early apoptotic, and late/necrotic cells in the dot plot. The percentage of apoptotic

cells after treatment with various concentrations of AgNPs were presented. Triplicate sets of experiment were examined.

JC-1 mitochondria membrane potential (MMP) assay

As mitochondria are the central regulators of the intrinsic apoptotic pathway, we determined the collapse in MMP in TDSCs after treatment with AgNPs using JC-1 staining^{33,34}. TDSCs were treated with AgNPs (0-150 µg/ml) for 6 h, washed and then stained with JC-1 (5 µg/ml) for 15 min in dark. After washing twice with PBS, the red and green fluorescent signals of JC-1 of 10,000 cells in each group were analyzed by flow cytometry. Valinomycin (10 µg/ml) was used to dissipate the MMP in the TDSCs in the positive control³⁵. Percentages of TDSCs and their intensities of green and red fluorescence emitted were determined. Triplicate sets of experiment were examined.

CM-H₂DCFDA cellular oxidative stress detection assay

To measure the oxidative stress after AgNP treatment, TDSCs were exposed to AgNPs (0-150 µg/ml) for 6 h and washed with PBS before trypsinization. The cells were then treated with CM-H₂DCFDA in PBS (5 µM) for 15 min and 10,000 cells in each group were analyzed by flow cytometry. TDSCs treated with hydrogen peroxide (H₂O₂, 0.03%), which induces ROS production, was used as a positive control (Wijeratne et al. 2005). Percentages of cell with high green fluorescence intensity were determined. Triplicate sets of experiment were examined.

Role of ROS in the cytotoxicity of AgNPs

To determine the role of ROS in mediating the cytotoxicity of AgNPs, TDSCs were pretreated with the antioxidant N-acetyl-L-cysteine (NAC) (10 mM) for 30 min at 37°C, 5% CO₂. Then, the cells were treated with AgNPs (75 & 150 µg/ml, the concentrations which showed increase in apoptosis, decrease in MMP or increase in cellular oxidative stress), followed by the apoptotic assay, MMP assay and cellular oxidative assay as described. Triplicate sets of experiment were examined.

Effects of sublethal doses of AgNPs on the proliferation, clonogenicity and tenogenic gene expression

[³H]-thymidine incorporation assay

TDSCs were plated at 2,000 cells per 96-well overnight and treated with AgNPs (0-15 µg/ml, below 18.8 µg/ml) in DMEM containing 1 µCi [³H]-thymidine (PerkinElmer, MA, USA) for 2 days at 37°C, 5% CO₂. The [³H]-thymidine incorporated into the DNA was then measured using a cell harvester and a liquid scintillation counter (Packard, TopCount NXTTM microplate scintillation and luminescence counter, PerkinElmer, MA, USA)^{9,10}. The percentage of [³H]-thymidine incorporation was calculated as $[(\text{CPM}_{\text{experimental}} - \text{CPM}_{\text{control}}) / \text{CPM}_{\text{control}}] \times 100\%$. Triplicate sets of experiment were examined.

Colony forming assay

The effect of sublethal doses of AgNPs (0-15 µg/ml, below 18.8 µg/ml) on the clonogenicity of TDSCs was assessed using the crystal violet staining method as described⁸. Briefly,

TDSCs were plated at 10 cells/cm² in 6-well plates, which was a suggested seeding density to allow stem cells to form colonies³⁶. Different concentrations of AgNPs were then added and the cells were cultured at 37°C, 5% CO₂ for 9 days. After washing with PBS, the cell colonies were stained with crystal violet (0.5 %, w/v) (Sigma, St. Louis, MO, USA). Colonies with diameter larger than 2 mm were counted and the results were presented in a bar chart^{8,9}. Triplicate sets of experiment were examined.

Quantitative real-time polymerase chain reaction (qRT-PCR) analysis of tendon-related markers

The effect of sublethal doses of AgNPs (0-15 µg/ml, below 18.8 µg/ml) on the expression of tendon-related markers in TDSCs were measured using qRT-PCR in triplicate as described⁹. Briefly, TDSCs (4,000 cells/cm²) were seeded in 6-well plates. When the cell culture reached confluence, AgNPs were added for 14 days and the RNA was extracted using the RNase mini kit (Qiagen, Hilden, Germany). The mRNA was reversely transcribed to complementary DNA (cDNA) using the First Strand cDNA Kit (Promega, Madison, WI, USA). Subsequently, the cDNA from each sample (0.2 µg) was amplified in a 25 ml reaction mixture containing the Platinum SYBR Green qPCR SuperMix-UDG and the specific primers for tendon-related gene markers including tenomodulin (*Tnmd*), scleraxis (*Scx*), collagen type 1 alpha-1 (*Col1A1*), collagen type 3 alpha-1 (*Col3A1*) or the house-keeping gene β-actin. The primer sequences and the gene product sizes are listed in Table. 1. The cycling conditions for qRT-PCR were shown as follows: denaturation at 95°C for 10 min, 45 cycles at 95°C for 20 sec, optimal annealing temperature for 25 sec, 72°C for 30 sec, and 60°C to 95°C with a heating rate of 0.1°C/sec. The mRNA level of the target gene was normalized to that of the β-actin. The relative gene expression was calculated using the 2^{-ΔΔ}

CT formula. The fold changes of gene expression in the experimental group relative to the gene expression in the control group were presented. Triplicate sets of experiment were examined.

Table. 1. The primer sequences and the gene product sizes of beta-actin, tenomodulin, scleraxis, collagen type 1 α 1 and Collagen type 3 α 1.

Table. 1. Primer sequences for qRT-PCR				
Genes	Accession number	Primer nucleotide sequence	Product size (bp)	Annealing temperature (°C)
Beta-actin (<i>β-actin</i>)	NM_03114 4.2	5'- ATCGTGGGCCGCCCTAGG CA-3'(Forward) 5'- TGGCCTTAGGGTTCAGAG GGG-3'(Reverse)	243	52
Tenomodulin (<i>Tnmd</i>)	NM_02229 0.1	5'- GTGGTCCCACAAGTGAAG GT-3'(Forward) 5'- GTCTTCCTCGCTTGCTTGT C-3' (Reverse)	60	52
Scleraxis (<i>Scx</i>)	NM_00113 0508.1	5'- AACACGGCCTTCACTGCG CTG-3'(Forward) 5'- CAGTAGCACGTTGCCAG GTG-3' (Reverse)	102	58
Collagen type 1 α 1 (<i>Col1A1</i>)	NM_05335 6.1	5'-CATCGGTGGTACTAAC- 3'(Forward) 5'- CTGGATCATATTGCACA- 3' (Reverse)	238	50
Collagen type 3 α 1 (<i>Col3A1</i>)	NM_03208 5.1	5'-GATGGCTGCACTAAAC- 3' (Forward) 5'- CGAGATTAAAGCAAGAG- 3' (Reverse)	225	50

Statistical analysis

WinMDI software was used for data analysis of flow cytometric assays. IBM SPSS software was used for statistical analysis. Statistical difference between experimental set and control set was expressed as mean \pm SD from at least three determinations. One-Way ANOVA was used to compare the mean difference between groups when the number of groups was more than two. Then post hoc Turkey test was used to tell specifically whether the control group and the treatment group significantly differed from each other. On the other hand, two independent T test was used to compare the mean difference between two groups. *p* values less than 0.05 were considered statistically significant.

Results & discussion

Physiochemical properties of AgNPs

It has been suggested that the cytotoxic and anti-bacterial effects of AgNPs are related to their physical and chemical features including sizes, shapes and coating agents^{37,38}. The risk and safe use of AgNPs for human health and environmental protection are still a controversial issue. Some previous studies claimed that AgNPs were harmless to cells²¹ but other studies indicated they were cytotoxic³⁹. These paradoxical results could be due to the different types of AgNPs they possessed and therefore characterization of AgNPs was vitally necessary. In our study, decahedral AgNPs coated with PVP were synthesized with 28.3 nm in edge length and 43.5 nm in diameter (Fig. 1a & 1b). The average hydrodynamic size of AgNPs is 54.8 nm in water and 71.0 nm in DMEM (Figure 1c). The hydrodynamic sizes are always larger than that of TEM imaging because of liquid medium. Water and protein molecules were attached to the nanoparticle due to the electric dipole force on the surface of nanoparticles⁴⁰. Also, DLS is an accurate tool to demonstrate the agglomeration of nanoparticles. Our AgNPs did not have agglomeration in both water and complete DMEM as only one single peak of AgNPs was detected. More importantly, intensity of peak absorbance at 495 nm was positively correlated with the concentration of AgNPs suspended with DMEM in the UV-visible spectrometric analysis (Fig. 1d). This implied that our PVP-coated AgNPs were stable and dispersed in complete medium with less particle agglomeration (Fig. 1c & 1d). Similar properties in other PVP-coated AgNPs have been reported⁴¹.

Fig. 1a

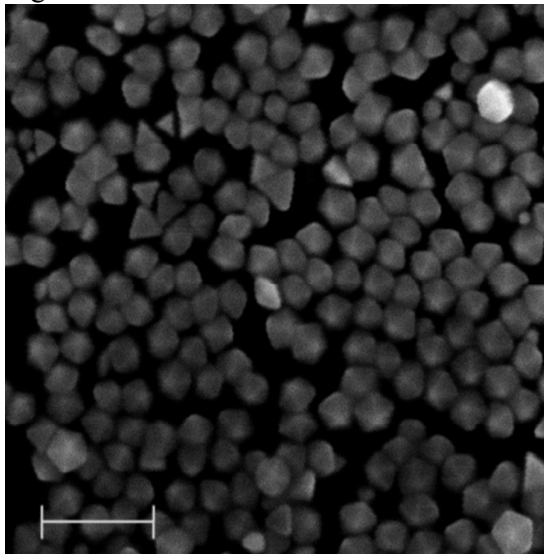


Fig. 1b

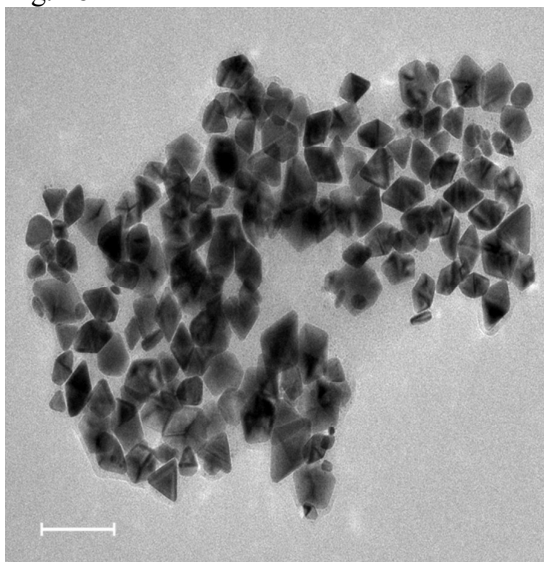


Fig. 1c

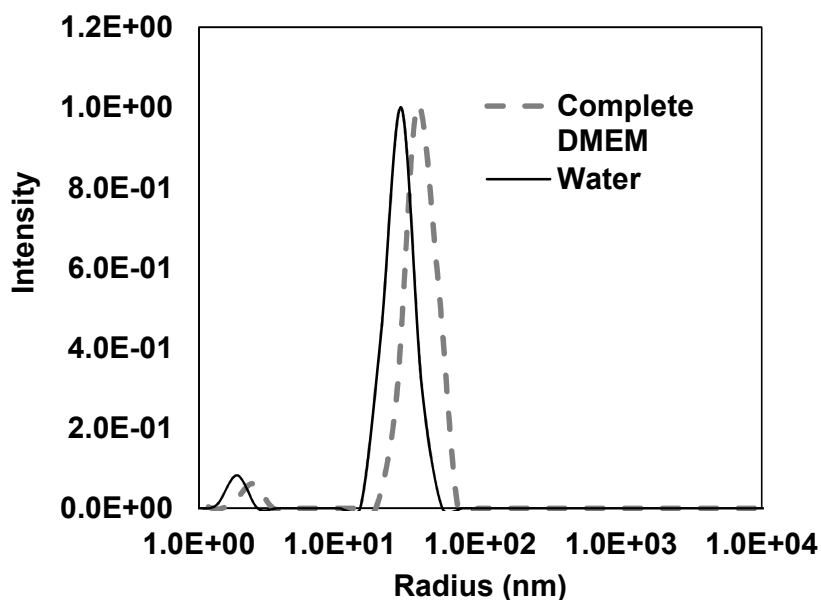


Fig. 1d

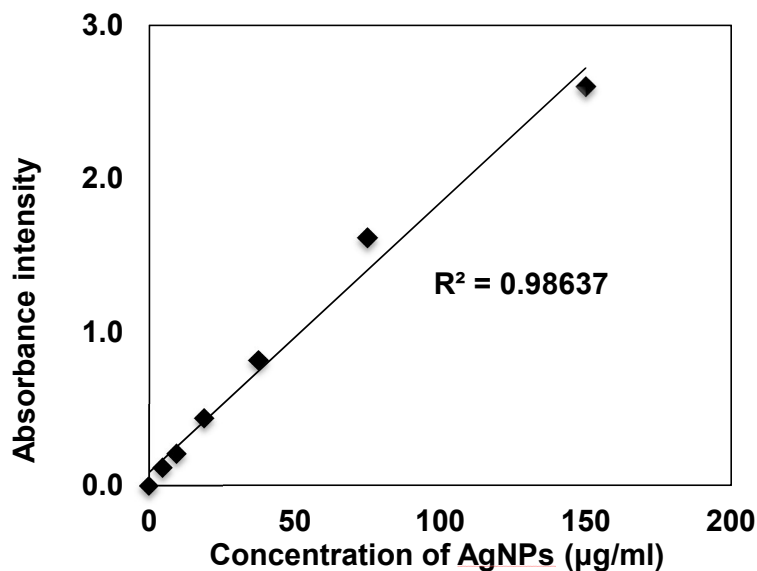


Fig. 1. Decahedral AgNPs were highly uniform. (a) High-resolution scanning electron microscope image of AgNPs. Scale bar: 200 nm. (b) High-resolution transmission electron microscopic image of AgNPs. Scale bar: 100 nm. (c) Dynamic light scattering for characterization of particles' size and distribution in water and complete medium (d) Positive linear relationship between different concentrations of AgNPs in DMEM containing 10% (v/v) FBS and 1% (v/v) P-S and the corresponding peak absorbance intensity at 495 nm.

AgNPs were cytotoxic to TDSCs at very high concentrations but relatively harmless at low concentrations

Regarding the results from MTT assay and morphological observations, cytotoxicity of AgNPs in TDSCs was found only when the concentrations were higher than 37.5 $\mu\text{g/ml}$ while AgNPs at the concentration below 18.8 $\mu\text{g/ml}$ did not affect TDSCs' viability (Fig. 2a & 2b). Similar to the IC_{50} of other PVP-coated AgNPs, the IC_{50} of our AgNPS was found to be 60 $\mu\text{g/ml}$ in the TDSCs³⁷. On the contrary, silver nitrate (AgNO_3) exhibited a robust cytotoxic effect. AgNO_3 concentration as low as 9.4 $\mu\text{g/ml}$ was able to kill almost all the TDSCs (Fig.2a). Similar situation was reported in human mesenchymal stem cells⁴². Given that release of silver ions from AgNPs may be the source of cytotoxicity⁴³ and the mass of our AgNPs refers to the mass of silver in the nanoparticle, findings in the present study therefore indicate 1) our AgNPs was less toxic than the silver ions alone at the same concentration and 2) PVP has executed its coating stabilizer task to reduce the release of silver ions from AgNPs and keep the nanoparticles dispersed effectively as mentioned by other studies⁴⁴⁻⁴⁶. In fact, the IC_{50} value of our PVP-coated AgNPs was found higher than that of AgNPs, with similar size, without PVP coating⁴⁷.

Fig. 2a

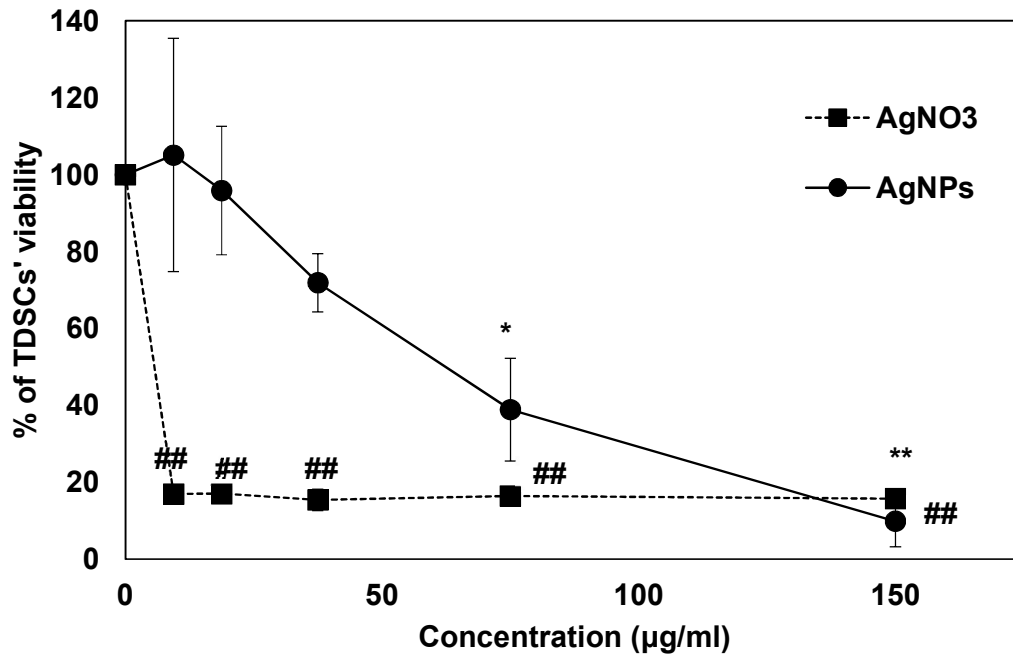


Fig. 2b

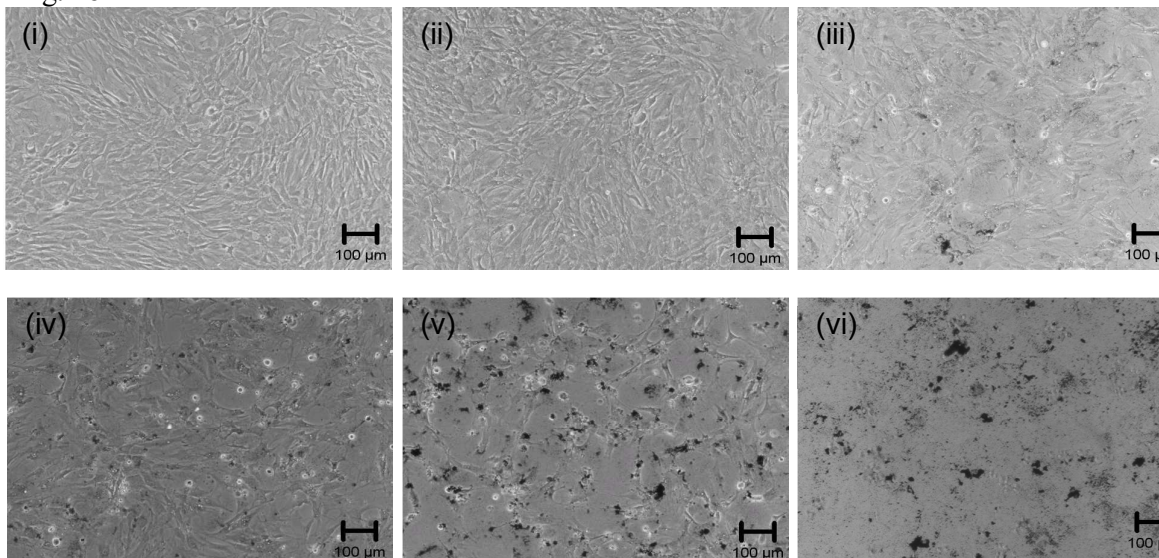


Fig. 2. Effects of AgNPs on the viability of TDSCs. (a) TDSCs (10^4 cells/well) were incubated with AgNPs or AgNO₃ at the indicated concentration at 37°C, 5% CO₂ for 24 h. Cell viability was then determined by the MTT assay. Results were shown as mean \pm SD (n = 3). **, ## $p < 0.01$; * $p < 0.05$ compared with control. (b) Morphological change of TDSC after incubation with different doses of AgNPs for 24 h. (i). Control. (ii). AgNPs (9.4 µg/ml).

(iii). AgNPs (18.8 $\mu\text{g/ml}$) (iv). AgNPs (37.5 $\mu\text{g/ml}$). (v). AgNPs (75 $\mu\text{g/ml}$). (vi). AgNPs (150 $\mu\text{g/ml}$). Scale bar: 100 μm .

The AgNPs-induced intrinsic apoptosis in TDSCs was mediated by oxidative stress and it could be prevented by using antioxidant

Regarding the results from MTT assay, we divided the concentrations into the lethal range (above 37.5 $\mu\text{g/ml}$) and sublethal range (below 18.8 $\mu\text{g/ml}$). Although AgNPs are reported to possess significant cytotoxic effects in some cells *in vitro*, it was unknown whether the same toxic mechanism existed in TDSCs. To this end, following a flow cytometric method in literature to determine the change in SSC for the uptake of AgNPs³², we found there was a significant uptake of AgNPs into TDSCs in a dose-dependent manner (Fig. 3). One of the limitations using this method to estimate the cellular uptake of AgNPs is that we could not eliminate the apoptogenic effect of AgNPs as apoptotic blebbing might also contribute to the change in the SSC. Nevertheless, this method clearly illustrated the correlation between the degrees of uptake with the concentrations of AgNPs applied. The mechanism for the uptake of AgNPs into TDSCs was also not clear but it might be mediated through energy-dependent endocytosis as AgNPs of similar size (50 nm) was reported to be internalized by non-phagocytic cells through endocytic processes^{48,49}. As can be seen, AgNPs were able to induce apoptosis (Fig. 4a), mitochondrial membrane depolarization (Fig. 4b) and ROS formation (Fig.5a) in a dose-dependent manner in the TDSCs. At the very high concentration of 150 $\mu\text{g/ml}$, AgNPs significantly induced early and late apoptosis ($93.2 \pm 2.7\%$ of the population) and loss of MMP ($77.9 \pm 13.6\%$ of the population) (Fig. 4a & 4b). Consistent with our previous observation in the MTT assay, AgNPs at the dose lower than 37.5 $\mu\text{g/ml}$ showed low apoptogenic effect in the TDSCs. At high concentration (150 $\mu\text{g/ml}$), AgNPs induced apoptosis of TDSCs via the activation of mitochondrial intrinsic pathway. Moreover,

oxidative stress was pronounced when the TDSCs were incubated with high doses of AgNPs (Fig. 5a). This effect was suppressed with the addition of the antioxidant NAC (Fig. 5b). As a precursor for the formation of the endogenous antioxidant glutathione, NAC plays an important role to maintain the intracellular glutathione level and to provide thiol group to counteract the oxidative stress^{50,50}. It is therefore not surprising that NAC could antagonize the AgNPs-induced loss of MMP and apoptosis (Fig. 5c-5d). Our results thus corroborated other work that the AgNP-induced cytotoxicity in mammalian cells is mediated via the induction of oxidative stress⁵¹ by increasing ROS²⁵, and eventually leading to apoptosis^{39,52,53}. Yet, which component of AgNPs causing the cytotoxic effects has been still under debate. It could be mediated by the released silver ions⁵⁴, nanoparticles alone⁵⁵, or both⁵⁶. In this circumstance, release of silver ions was speculated since previous group has demonstrated the “Trojan horse effect” about the release of intracellular silver ions after uptake of AgNPs⁵⁶.

Fig. 3

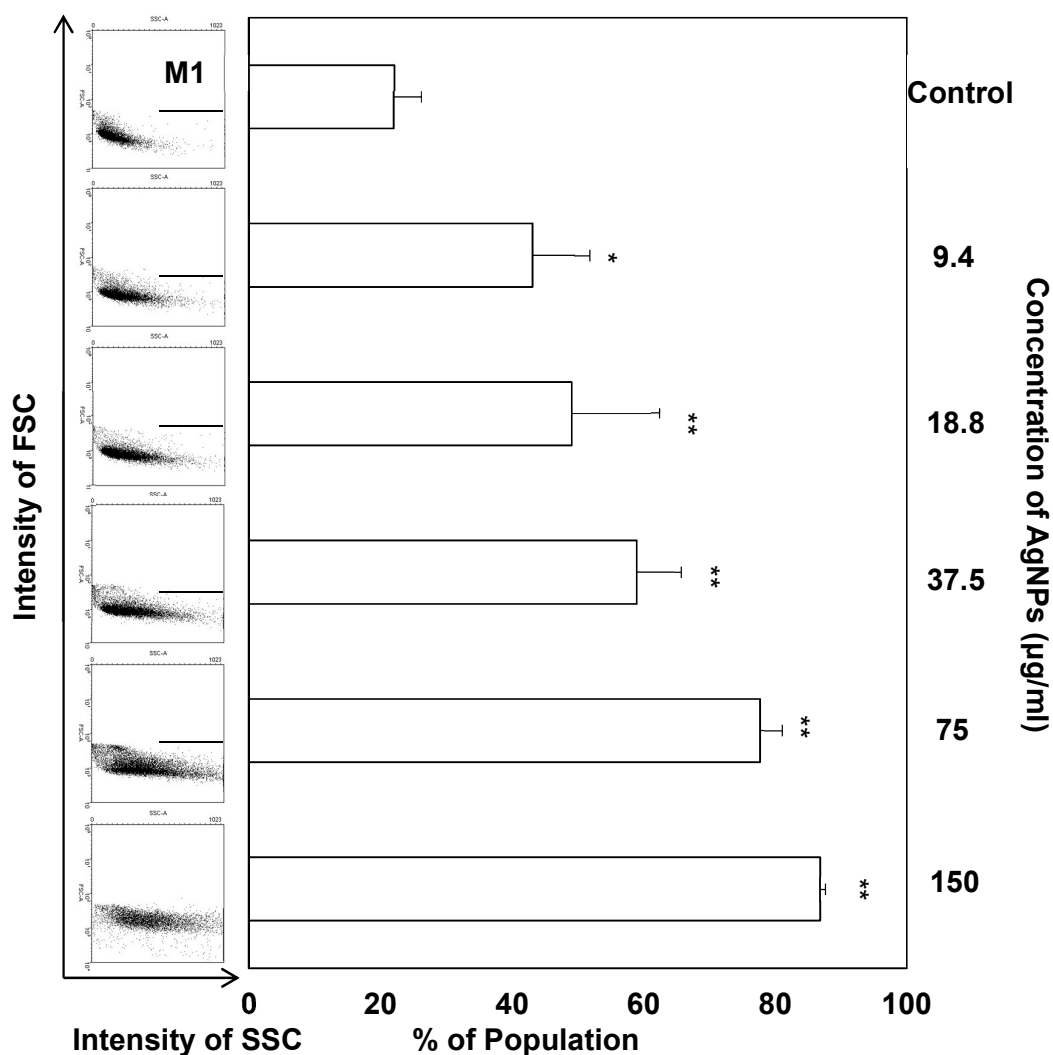


Fig. 3. Cellular uptake of AgNPs in TDSCs. TDSCs ($3 \times 10^4/\text{cm}^2$) were incubated with AgNPs at the indicated concentration at 37°C , 5% CO_2 for 24 h. The FSC and SSC signals were subsequently determined at single cell level by flow cytometry and the results were displayed in dot plots. The percentage of cells in the selected M1 region was measured and the results (mean \pm SD, $n = 3$) were shown in a bar chart. ** $p < 0.01$; * $p < 0.05$ compared with control.

Fig. 4a

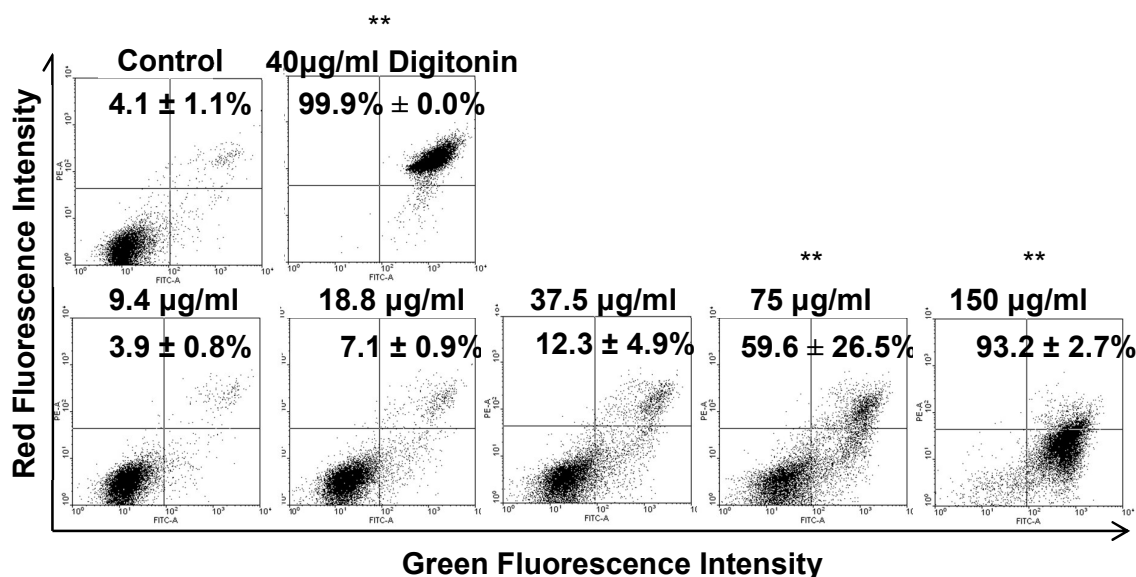


Fig. 4b

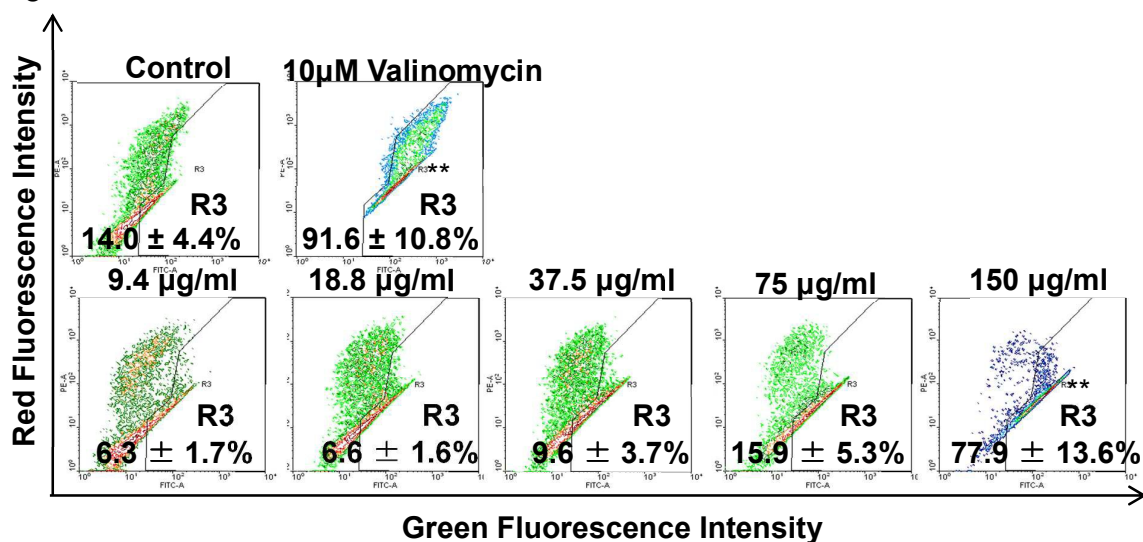


Fig. 4. Effect of AgNPs on the induction of apoptosis and depolarization of MMP in TDCs. (a) TDCs ($3 \times 10^4/\text{cm}^2$) treated with different concentrations of AgNP for 24 h were stained with annexin-V-GFP and PI. The percentages of apoptotic cells in the lower-right quadrant (annexin-V-GFP^{High}; PI^{Low}) and in the upper-right quadrant (annexin-V-GFP^{High}; PI^{High}) were counted. TDCs treated with digitonin (40 μg/ml) were used as a positive control. Results were shown as mean ± SD ($n = 3$). ** $p < 0.01$; * $p < 0.05$ compared with control. (b) TDCs ($3 \times 10^4/\text{cm}^2$) treated with different concentrations of AgNP for 6 h were stained with JC-1. Valinomycin (10 μg/ml) was used as a positive control. The percentages of cells with dissipation of MMP (lower-right quadrant) were presented as mean ± SD ($n = 3$). ** $p < 0.01$ compared with control.

Fig. 5a

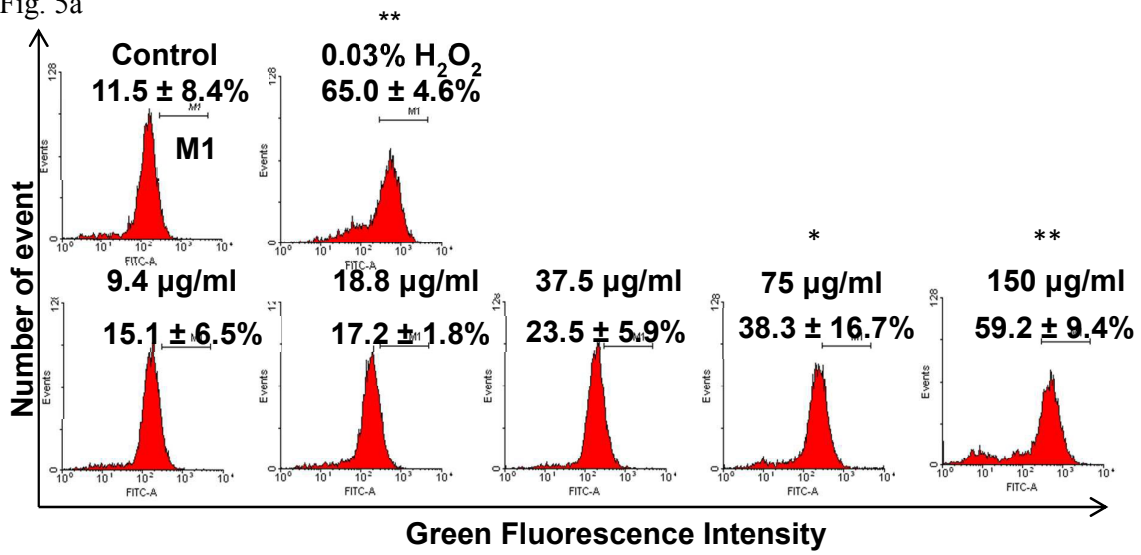


Fig. 5b

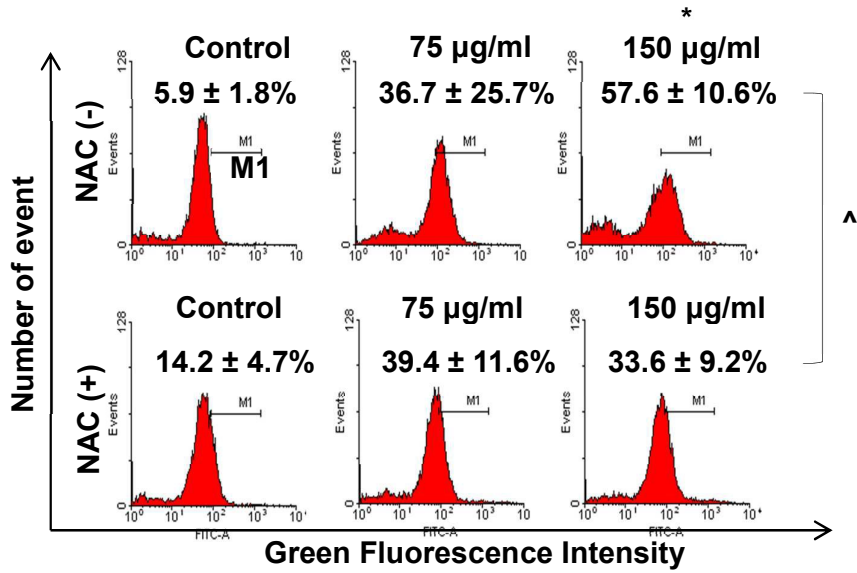


Fig. 5c

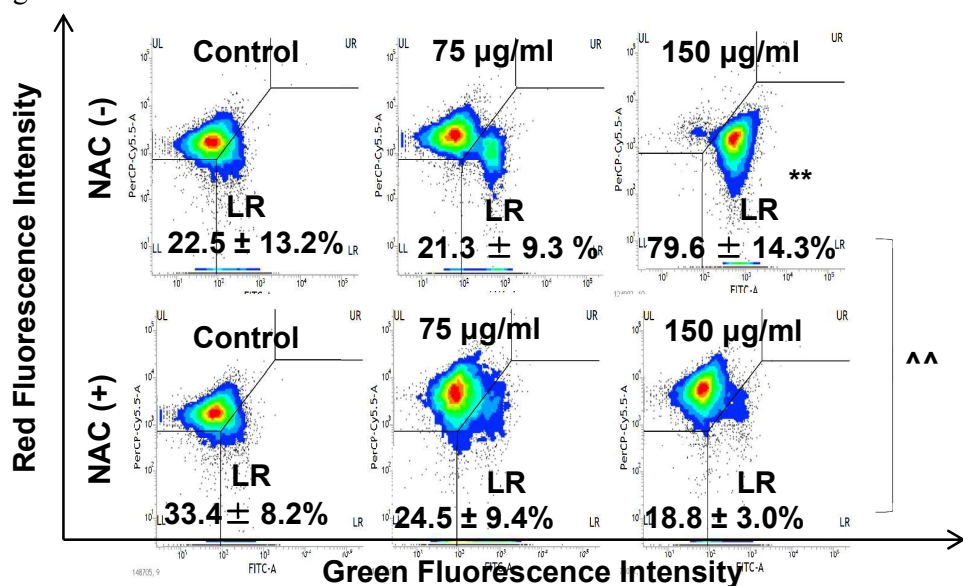


Fig. 5d

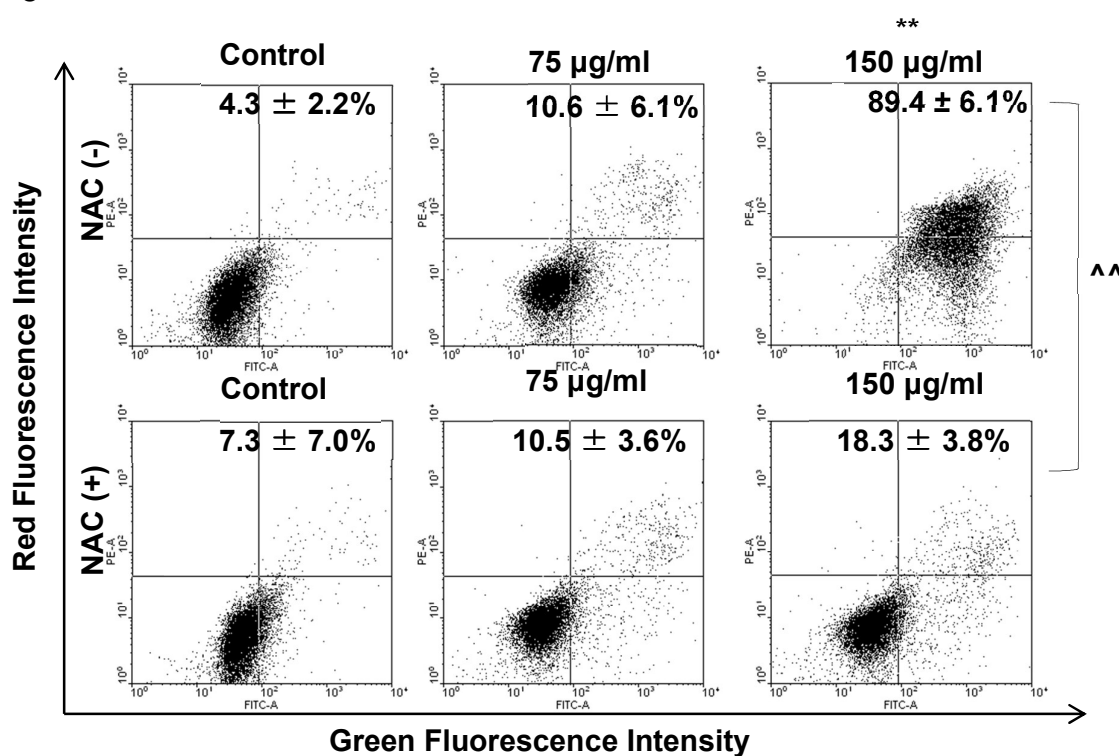


Figure 5. Effect of AgNPs on ROS production and effect of NAC in AgNPs-induced cytotoxicity. (a) TDCs ($3 \times 10^4/\text{cm}^2$) were incubated with 0-150 µg/ml AgNPs for 6 h and stained with CM-H₂DCFDA. The percentages of cell population in strong green fluorescence was determined. Results were presented as mean ± SD for three determinations. ** $p < 0.01$; * $p < 0.05$ compared with control. TDCs were pre-treated with 10 mM NAC for 30 min before the exposure to AgNPs (75, 150 µg/ml) for 6 h (b) ROS and (c) MMP assays and (d)

24 h annexin-V and PI assay. The percentages of cells with change in fluorescence intensity were shown. Results were shown as mean \pm SD for three determinations. **, ## $p < 0.01$; *, # $p < 0.05$ compared with the control. ^^ $p < 0.01$; ^ $p < 0.05$ compared with the corresponding value between the NAC-treated group and normal group.

Sublethal AgNPs inhibited TDSCs' proliferation dose-dependently

A very recent review has indicated that there have been very few investigations studying the sublethal effects of AgNPs under the low-dosed exposure²⁸. Despite this, the low concentrations of AgNPs could better assess or estimate the health hazards of AgNPs used in medical application⁴⁷ and AgNPs exposed under environmental conditions²⁸. More importantly, the sublethal effects of AgNPs have been shown differently when compared with the acute cytotoxic effects of AgNPs at high concentrations. For instance, it was found that the polyethylenimine-coated AgNPs (7-10 nm in size) accelerated cell proliferation and up-regulated proliferation-related genes at low concentrations below 0.5 $\mu\text{g/ml}$ ⁵⁷. Likewise, PVP-coated AgNPs (5-10 nm in size, shape not mentioned) at low doses were not cytotoxic to rat tendon primary cells and promoted rat tendon repair *in vivo*⁵⁸. Contrary to their findings, our decahedral PVP-coated AgNPs (43.5 nm in diameter) at low doses (0-15 $\mu\text{g/ml}$) blocked the proliferation and colony formation of TDSCs after a 2- and 9- day culture respectively (Fig. 6a & 6b). The inhibitory effects were dose-dependent and no stimulatory effect of proliferation was observed at concentrations lower than 0.5 $\mu\text{g/ml}$. The difference between studies may be due to different physicochemical properties of AgNPs mentioned above. Although we could not fully explain the dissimilarity, we successfully demonstrated the inhibitory effect of sublethal AgNPs. More importantly, many previous studies have only shown the toxicological data of AgNPs with one time point (e.g. 24 h). Our data suggested that AgNPs did exhibit detrimental impact on TDSCs at relatively low concentrations after

several days even though they were unable to cause acute toxic effects in cells' viability after 24 hours (Fig. 2a & 2b).

Fig. 6a

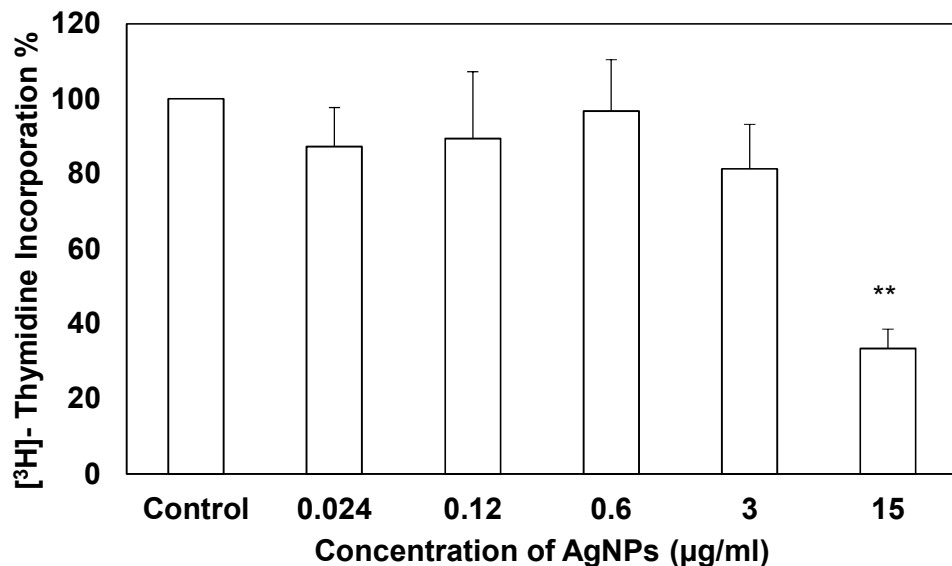


Fig. 6b

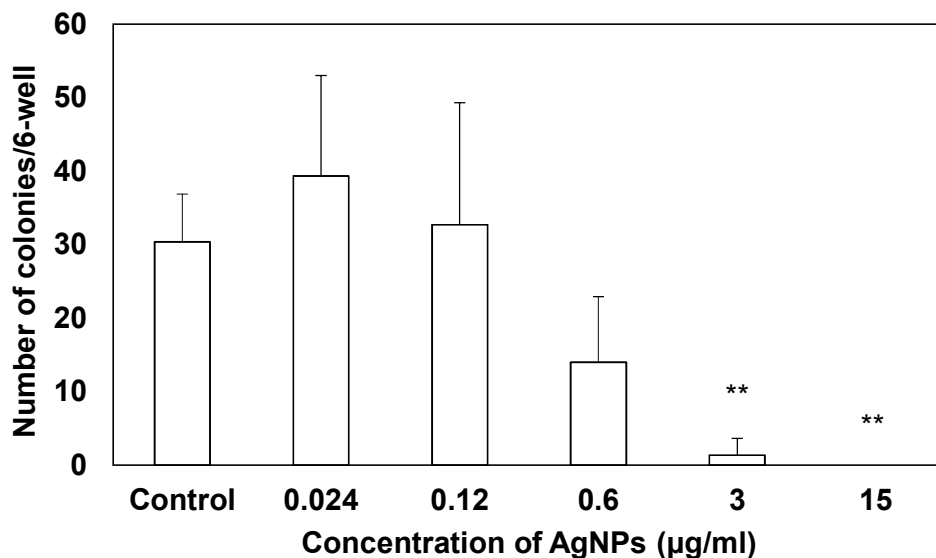


Fig. 6. Effects of AgNPs on cell proliferation and clonogenicity in TDSCs. TDSCs (2,000 cells per 96-well in cell proliferation assay; 10 cells/cm² per 6-well in clonogenicity assay) were incubated with AgNPs at the indicated concentrations at 37°C, 5% CO₂ for two days (cell proliferation assay) or nine days (clonogenicity assay). **(a)** Cell proliferative potential was determined by the [³H]-thymidine incorporation assay. Results were quantified as mean ± SD (n = 3). ** *p* < 0.01; * *p* < 0.05 compared with control. **(b)** Number of colonies was

determined by staining the cells with 0.5% crystal violet. Results were quantified as mean \pm SD (n = 3). ** $p < 0.01$; * $p < 0.05$ compared with control.

Sublethal AgNPs down-regulated the tenogenic markers of TDSCs

The inhibitory effects of AgNPs on stem cell differentiation have been reported in other literature. For example, PVP-coated AgNPs (50 nm in diameter, shape not mentioned) was reported to inhibit the osteogenic differentiation of murine primary osteoblasts⁵⁹ while some other studies documented that AgNPs (Bimetallic gold-core/silver-shell spherical nanoparticle with 10–20 nm in diameter) did not influence the osteogenic differentiation of human adipose-derived stem cells⁶⁰. However, there have been a lack of studies about nanomaterials' effect on tenogenic differentiation and therefore this study is the first of its kind to examine how sublethal AgNPs affect tenogenic differentiation of stem cells. Besides the collagen markers, tenomodulin and scleraxis were also used for evaluation as they are specific tenogenic differentiation markers^{8,61}. Scleraxis is a basic helix–loop–helix transcription factor that is expressed in early tendon progenitor cells and kept expressed during the tendon development. The expression of scleraxis is also crucial to tenogenic regulation because scleraxis-null mutant mice have shown severe defects in tendon development and force transmission⁶² while scleraxis-transduced TDSCs promote better tendon repair than normal TDSCs⁶³. On the other hand, tenomodulin is a type II transmembrane glycoprotein⁶⁴ that has been identified as a marker of tendon differentiation⁶⁵ and positively regulated by scleraxis⁶⁶. Regarding the differentiation assays, our data indicated that AgNPs dose-dependently suppressed the mRNA expression of tendon-related markers in TDSCs when compared to that of the untreated control after treatment for 14 days

(Fig. 7a-7d). Unlike the previous studies, our AgNPs down-regulated gene expressions instead of up-regulating them. The reason why different types of AgNPs have different effects on differentiation in stem cells remains unknown. Their sizes, shapes and coatings may be some of the critical factors. Future work is needed to have a better understanding in this regard.

Fig. 7a

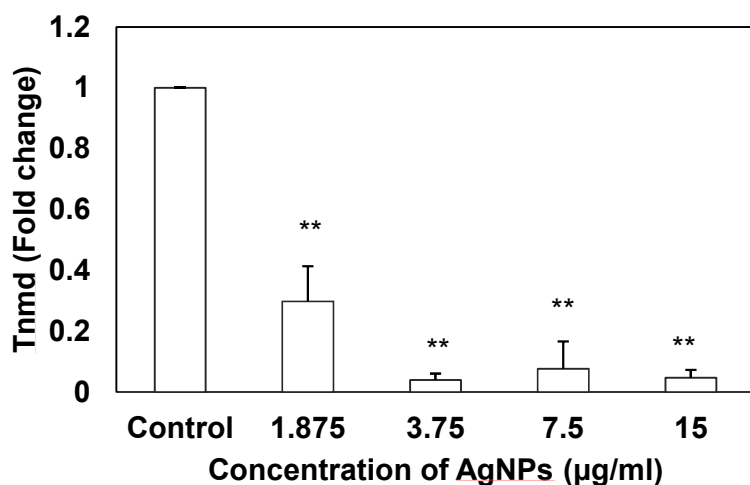


Fig. 7b

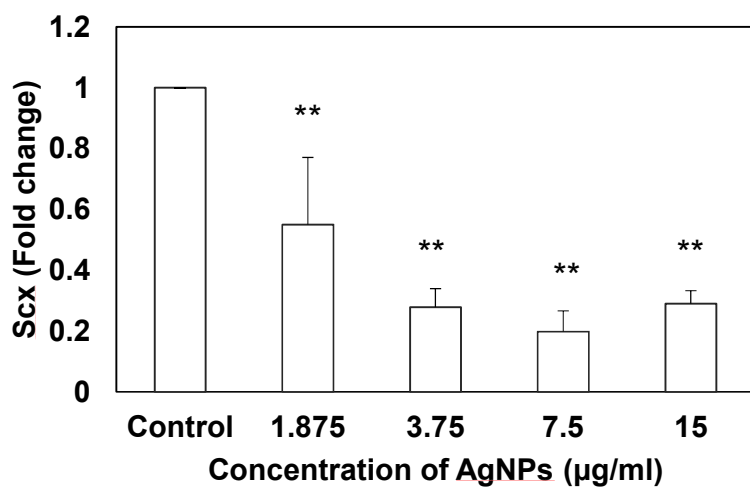


Fig. 7c

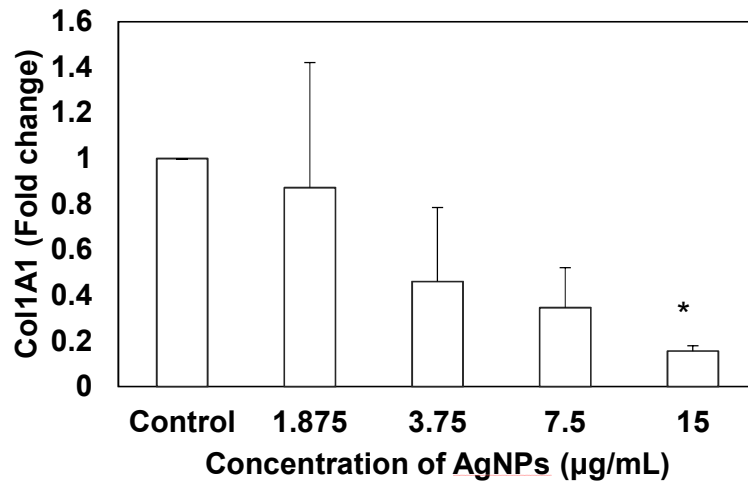


Fig. 7d

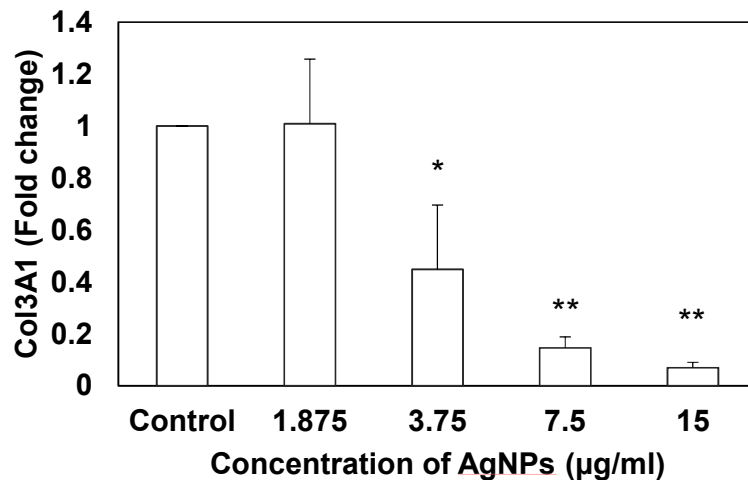


Fig. 7. Effects of AgNPs on the expression of tendon-related markers in TDSCs. TDSCs were incubated with AgNPs at the indicated concentration at 37°C, 5% CO₂ for 14 days. The mRNA levels of (a) *Tnmd*, (b) *Scx*, (c) *Col1A1* and (d) *Col3A1* were determined by RT-qPCR. The bar charts showed the fold changes of markers after normalization with β -actin. Results were presented as mean \pm SD, n = 3. ** $p < 0.01$ * $p < 0.05$ compared with control.

Conclusion

In conclusion, our data demonstrated that the decahedral AgNPs (43.5 nm in diameter) coated with PVP have cytotoxic effects beginning at 37.5 µg/ml. High dose of AgNPs (75-150 µg/ml) induced apoptosis in the TDSCs via the activation of ROS and mitochondrial intrinsic pathway as confirmed by PS externalization, loss of cell membrane integrity, decrease in the MMP and rise in intracellular ROS. Pretreatment of NAC could prevent the toxicity caused by AgNPs, even in high doses. Regarding the sublethal effects of AgNPs, low concentrations of AgNPs (below 18.8 µg/ml) did not provoke cytotoxicity to TDSCs in the 24-h viability assay. However, they exhibited inhibitory effects on proliferation, colony-formation and tendon-related marker expression in the TDSCs at the non-cytotoxic concentrations (0-15 µg/ml). Collectively, false to our expectation, AgNPs possessed detrimental effects at both cytotoxic and sublethal concentrations. Based on our observations, the PVP-coated decahedral AgNP was not a good scaffold fabrication material in tendon engineering. For a better use of AgNPs, more work should be done to evaluate the effects of AgNPs at sublethal dose on animals and humans.

Acknowledgement

This work is partially supported by the General Research Fund (project number: 471411) and Collaborative Research Fund (Project number: CUHK1/CRF/12G) from the Hong Kong Special Administrative Region.

References

- 1 P. Sharma and N. Maffulli, *J. Bone Joint Surg. Am.*, 2005, **87**, 187–202.
- 2 N. Maffulli, J. Wong and L. C. Almekinders, *Clin. Sports Med.*, 2003, **22**, 675–692.
- 3 S. Wang, C. Zinderman, R. Wise and M. Braun, *Cell Tissue Bank.*, 2007, **8**, 211–9.
- 4 Z. Yin, X. Chen, J. L. Chen, W. L. Shen, T. M. Hieu Nguyen, L. Gao and H. W. Ouyang, *Biomaterials*, 2010, **31**, 2163–75.
- 5 M. Young, *Stem Cells Int.*, 2012, 2012, 637836.
- 6 P. Lui and K. Chan, *Stem Cell Rev. Reports*, 2011, 883–897.
- 7 Y. Bi, D. Ehrchiou, T. M. Kilts, C. a Inkson, M. C. Embree, W. Sonoyama, L. Li, A. I. Leet, B.-M. Seo, L. Zhang, S. Shi and M. F. Young, *Nat. Med.*, 2007, **13**, 1219–27.
- 8 Y.-F. Rui, P. P. Y. Lui, G. Li, S. C. Fu, Y. W. Lee and K. M. Chan, *Tissue Eng. Part A*, 2010, **16**, 1549–58.
- 9 Q. Tan, P. P. Y. Lui, Y. F. Rui and Y. M. Wong, *Tissue Eng. Part A*, 2012, 18, 840–851.
- 10 P. P. Y. Lui, S. K. Kong, P. M. Lau, Y. M. Wong, Y. W. Lee, C. Tan and O. T. Wong, *Tissue Eng. Part A*, 2014, **20**, 3010–20.
- 11 P. P. Y. Lui, S. K. Kong, P. M. Lau, Y. M. Wong, Y. W. Lee, C. Tan and O. T. Wong, *Tissue Eng. Part A*, 2014, **20**, 2998–3009.
- 12 K. Chaloupka, Y. Malam and A. M. Seifalian, *Trends Biotechnol.*, 2010, **28**, 580–8.
- 13 M. Rai, A. Yadav and A. Gade, *Biotechnol. Adv.*, 2009, **27**, 76–83.
- 14 A. R. Shahverdi, A. Fakhimi, H. R. Shahverdi and S. Minaian, *Nanomedicine*, 2007, **3**, 168–71.
- 15 P. L. Nadworny, J. Wang, E. E. Tredget and R. E. Burrell, *Nanomedicine*, 2008, **4**, 241–51.
- 16 R. G. Sibbald, J. Contreras-Ruiz, P. Coutts, M. Fierheller, A. Rothman and K. Woo, *Adv. Skin Wound Care*, 2007, **20**, 549–58.
- 17 J. B. Wright, K. Lam, A. G. Buret, M. E. Olson and R. E. Burrell, *Wound Repair Regen.*, 2002, **10**, 141–51.
- 18 J. Tian, K. K. Y. Wong, C.-M. Ho, C.-N. Lok, W.-Y. Yu, C.-M. Che, J.-F. Chiu and P. K. H. Tam, *ChemMedChem*, 2007, **2**, 129–36.

- 19 D. Roe, B. Karandikar, N. Bonn-Savage, B. Gibbins and J.-B. Rouillet, *J. Antimicrob. Chemother.*, 2008, **61**, 869–76.
- 20 V. D’Britto, H. Kapse, H. Babrekar, a a Prabhune, S. V Bhoraskar, V. Premnath and B. L. V Prasad, *Nanoscale*, 2011, **3**, 2957–63.
- 21 V. Alt, T. Bechert, P. Steinrücke, M. Wagener, P. Seidel, E. Dingeldein, E. Domann and R. Schnettler, *Biomaterials*, 2004, **25**, 4383–91.
- 22 C. W. Li, R. Q. Fu, C. P. Yu, Z. H. Li, H. Y. Guan, D. Q. Hu, D. H. Zhao and L. C. Lu, *Int. J. Nanomedicine*, 2013, **8**, 4131–4145.
- 23 K. Karthikeyan, S. Sekar, M. P. Devi, S. Inbasekaran, C. H. Lakshminarasaiah and T. P. Sastry, *J. Mater. Sci. Mater. Med.*, 2011, **22**, 2721–6.
- 24 Y. Li, J. a Bhalli, W. Ding, J. Yan, M. G. Pearce, R. Sadiq, C. K. Cunningham, M. Y. Jones, W. a Monroe, P. C. Howard, T. Zhou and T. Chen, *Nanotoxicology*, 2013, **5390**, 1–10.
- 25 Y.-H. Hsin, C.-F. Chen, S. Huang, T.-S. Shih, P.-S. Lai and P. J. Chueh, *Toxicol. Lett.*, 2008, **179**, 130–9.
- 26 P. V Asharani, M. P. Hande and S. Valiyaveetil, *BMC Cell Biol.*, 2009, **10**, 65.
- 27 C. M. Powers, A. R. Badireddy, I. T. Ryde, F. J. Seidler and T. A. Slotkin, *Environ. Health Perspect.*, 2011, **119**, 37–44.
- 28 Z. Wang, T. Xia and S. Liu, *Nanoscale*, 2015, **7**, 7470–81.
- 29 B. Pietrobon and V. Kitaev, *Chem. Mater.*, 2008, **20**, 5186–5190.
- 30 M. Ni, P. P. Y. Lui, Y. F. Rui, Y. W. Lee, Y. W. Lee, Q. Tan, Y. M. Wong, S. K. Kong, P. M. Lau, G. Li and K. M. Chan, *J. Orthop. Res.*, 2012, **30**, 613–9.
- 31 N. A. Monteiro-Riviere, A. O. Inman and L. W. Zhang, *Toxicol. Appl. Pharmacol.*, 2009, **234**, 222–35.
- 32 M. Ghosh, M. J. S. Sinha, A. Chakraborty, S. K. Mallick, M. Bandyopadhyay and A. Mukherjee, *Mutat. Res.*, 2012, **749**, 60–9.
- 33 G. Kroemer and J. C. Reed, *Nat. Med.*, 2000, **6**, 513–9.
- 34 M. Reers, T. W. Smith and L. B. Chen, *Biochemistry*, 1991, **30**, 4480–6.
- 35 S. B. Hladky, J. C. Leung and W. J. Fitzgerald, *Biophys. J.*, 1995, **69**, 1758–72.
- 36 N. a P. Franken, H. M. Rodermond, J. Stap, J. Haveman and C. van Bree, *Nat. Protoc.*, 2006, **1**, 2315–2319.

- 37 T. Silva, L. R. Pokhrel, B. Dubey, T. M. Tolaymat, K. J. Maier and X. Liu, *Sci. Total Environ.*, 2014, **468-469**, 968–76.
- 38 M. I. Azócar, L. Tamayo, N. Vejar, G. Gómez, X. Zhou, G. Thompson, E. Cerda, M. J. Kogan, E. Salas and M. A. Paez, *J. Nanoparticle Res.*, 2014, **16**, 2465.
- 39 N. Miura and Y. Shinohara, *Biochem. Biophys. Res. Commun.*, 2009, **390**, 733–7.
- 40 J. H. Shannahan, X. Lai, P. C. Ke, R. Podila, J. M. Brown and F. A. Witzmann, *PLoS One*, 2013, **8**, e74001.
- 41 Y. Li, W. Zhang, J. Niu and Y. Chen, *Environ. Sci. Technol.*, 2013, **47**, 10293–10301.
- 42 C. Greulich, S. Kittler, M. Epple, G. Muhr and M. Köller, *Langenbeck's Arch. Surg.*, 2009, **394**, 495–502.
- 43 A. Pratsinis, P. Hervella, J.-C. Leroux, S. E. Pratsinis and G. A. Sotiriou, *Small*, 2013, **9**, 2576–84.
- 44 T. M. Tolaymat, A. M. El Badawy, A. Genaidy, K. G. Scheckel, T. P. Luxton and M. Suidan, *Sci. Total Environ.*, 2010, **408**, 999–1006.
- 45 R. Bryaskova, D. Pencheva, S. Nikolov and T. Kantardjiev, *J. Chem. Biol.*, 2011, **4**, 185–91.
- 46 A. M. El Badawy, K. G. Scheckel, M. Suidan and T. Tolaymat, *Sci. Total Environ.*, 2012, **429**, 325–31.
- 47 S. Chernousova and M. Epple, *Angew. Chem. Int. Ed. Engl.*, 2013, **52**, 1636–53.
- 48 J. Rejman, V. Oberle, I. S. Zuhorn and D. Hoekstra, *Biochem. J.*, 2004, **377**, 159–69.
- 49 W. Jiang, B. Y. S. Kim, J. T. Rutka and W. C. W. Chan, *Nat. Nanotechnol.*, 2008, **3**, 145–50.
- 50 C. Kerksick and D. Willoughby, *J. Int. Soc. Sports Nutr.*, 2005, **2**, 38–44.
- 51 M. J. Piao, K. A. Kang, I. K. Lee, H. S. Kim, S. Kim, J. Y. Choi, J. Choi and J. W. Hyun, *Toxicol. Lett.*, 2011, **201**, 92–100.
- 52 M. Jeyaraj, M. Rajesh, R. Arun, D. MubarakAli, G. Sathishkumar, G. Sivanandhan, G. K. Dev, M. Manickavasagam, K. Premkumar, N. Thajuddin and A. Ganapathi, *Colloids Surf. B. Biointerfaces*, 2013, **102**, 708–17.
- 53 N. Ucciferri, E.-M. Collnot, B. K. Gaiser, A. Tirella, V. Stone, C. Domenici, C.-M. Lehr and A. Ahluwalia, *Nanotoxicology*, 2014, **8**, 697–708.
- 54 C. Beer, R. Foldbjerg, Y. Hayashi, D. S. Sutherland and H. Autrup, *Toxicol. Lett.*, 2012, **208**, 286–92.

- 55 K. Kawata, M. Osawa and S. Okabe, *Environ. Sci. Technol.*, 2009, **43**, 6046–51.
- 56 E.-J. Park, J. Yi, Y. Kim, K. Choi and K. Park, *Toxicol. In Vitro*, 2010, **24**, 872–8.
- 57 K. Kawata, M. Osawa and S. Okabe, *Environ. Sci. Technol.*, 2009, **43**, 6046–51.
- 58 K. H. L. Kwan, K. W. K. Yeung, X. Liu, K. K. Y. Wong, H. C. Shum, Y. W. Lam, S. H. Cheng, K. M. C. Cheung and M. K. T. To, *Nanomedicine*, 2014, **10**, 1375–83.
- 59 C. E. Albers, W. Hofstetter, K. a Siebenrock, R. Landmann and F. M. Klenke, *Nanotoxicology*, 2013, **7**, 30–6.
- 60 M. E. Samberg, E. G. Lobo, S. J. Oldenburg and N. A. Monteiro-Riviere, *Nanomedicine (Lond)*, 2012, **7**, 1197–209.
- 61 P. P. Y. Lui, Y. F. Rui, M. Ni and K. M. Chan, *J. Tissue Eng. Regen. Med.*, 2011, **5**, e144–63.
- 62 N. D. Murchison, B. a Price, D. a Conner, D. R. Keene, E. N. Olson, C. J. Tabin and R. Schweitzer, *Development*, 2007, **134**, 2697–708.
- 63 C. Tan, P. P. Y. Lui, Y. W. Lee and Y. M. Wong, *PLoS One*, 2014, **9**, e97453.
- 64 O. Brandau, A. Meindl, R. Fässler and A. Aszódi, *Dev. Dyn.*, 2001, **221**, 72–80.
- 65 D. Docheva, E. B. Hunziker, R. Fässler and O. Brandau, *Mol. Cell. Biol.*, 2005, **25**, 699–705.
- 66 C. Shukunami, A. Takimoto, M. Oro and Y. Hiraki, *Dev. Biol.*, 2006, **298**, 234–47.

A table of contents entry

First study evaluating the full range of dose-response relationship between decahedral silver nanoparticles and rat tendon-derived stem cells

